Check for updates

Dendrimer-conjugated podophyllotoxin suppresses DENA-induced HCC progression by modulation of inflammatory and fibrogenic factors†

Supriya Sharma,[a,c] Mehak,[b] Jyoti Chhimwal,[a,c] Vikram Patial ID *[a,c] and Ugir Hossain Sk*[b,d]

Podophyllotoxin has been explored as an anticancer, antiviral, and antibacterial agent; however, its low water solubility and toxicity limit its use. In this study, the efficacy of a more soluble and less toxic poly-amidoamine (PAMAM) dendrimer-conjugated podophyllotoxin (DPODO) was evaluated against chemically induced hepatocellular carcinoma (HCC) in mice. HCC was induced by giving 0.01% diethyl-nitrosamine (DENA) in drinking water for 16 weeks. The HCC-induced mice were treated with 10 or 20 mg per kg body weight DPODO. The DENA administration led to HCC development, characterized by anisocytosis, karyomegaly, inflammation and degenerative changes in the liver. The DPODO treatment at 10 mg and 20 mg doses significantly reduced the histopathological changes in liver tissue. The DPODO treatment also significantly lowered the levels of inflammatory markers IL-6 and NF-κB in serum and tissue, respectively. Further, the treatment also significantly reduced fibrous tissue deposition in the liver, which was further confirmed by the reduced mRNA levels and tissue expression of fibrogenic markers TGF-β and α-SMA in the liver. The results of the present study indicate that DPODO treatment suppresses the progression of HCC by modulating the inflammatory and fibrogenic factors, which play important roles in HCC development.

1. Introduction

Liver cancer is estimated to be the fifth most common cancer globally, accounting for up to 80% of all cancer cases.[1] The increasing incidence of hepatocellular carcinoma (HCC) makes it the second leading cause of death.[2] The prime factors responsible for HCC include viral infection (hepatitis B and C), the consumption of mycotoxin-contaminated food grains, industrial toxicants, and excessive consumption of alcohol.[3] DENA is a commonly used carcinogen for investigating the progression of HCC in experimental animals. It is one of the environmental toxicants present in cosmetics, tobacco smoke,

and processed dairy and meat products.[4] DENA acts by producing nitric oxide (NO), leading to hypoxic tissue condition, suppression of deoxyribonucleotide synthesis, and thus disturbing protein synthesis.[5] Aggressive treatment strategies for liver cancer are limited, and the development of drug resistance makes HCC treatment a great challenge.[1] Further, the prognosis of the disease remains poor due to the high rates of hepatic carcinoma relapse. Chemotherapy is one of the approaches to cure HCC, but the use of chemotherapeutic agents is also associated with many harmful effects, routing towards mortality.[6]

Podophyllotoxin is a naturally occurring cyclolignan synthesized through the shikimic acid pathway and mainly isolated from *Podophyllum peltatum* Linn. and *P. hexandrum*. It possesses anticancer and immunosuppressive properties, along with antiviral effects against influenza, warts, and herpes viruses.[7] However, due to its toxic side effects, extensive structural modifications have been performed on the compound over the years.[8] Etoposide, one of the derivatives of podophyllotoxin, has been reported to have high therapeutic activity, especially in the treatment of leukemia, malignant lymphoma and testicular carcinoma.[9] It has been reported to reversibly bind with tubulin, preventing microtubule for-

[a]*Pharmacology and Toxicology Laboratory, Institute of Himalayan Bioresource Technology, Palampur, H.P., India. E-mail: vikrampatial@ihbt.res.in, drvikrampatial@yahoo.in*
[b]*Natural Products Chemistry and Process Development Division, Institute of Himalayan Bioresource Technology, Palampur, H.P., India*
[c]*Academy of Scientific & Innovative Research, Institute of Himalayan Bioresource Technology, Palampur, H.P., India*
[d]*Clinical and Translational Research, Chittaranjan National Cancer Institute, Kolkata 700026, India. E-mail: uhocju@gmail.com*
†Electronic supplementary information (ESI) available. See DOI: 10.1039/c9tx00103d

mation and inducing apoptosis.[10] In the previous studies, etoposide is reported to be active against HCC; however, the escalation of etoposide dosage is impossible in patients with HCC due to the toxicity of the drug.[11,12] Its low hydrophilicity and the resulting drug resistance and drastic gastrointestinal aberrations have led to the exploration of new derivatives of podophyllotoxin.

Dendrimer-like macromolecules are used as efficient carriers for drug delivery. Dendrimer-conjugated drugs have the potential to improve drugs' aqueous solubility, stability, circulation time, passive targeting to tumours, and movement across biological barriers.[13–16] The commercially available PAMAM and polypropylenimine (PPI) dendrimers are the most widely used in biomedical applications and drug delivery because of their capability to cross cell membranes by endocytosis.[10,13,17–19] Maltose-modified PPI dendrimers have been used to exert immunomodulatory effect at specific sizes, whereas the PAMAM dendrimers are being used for siRNA delivery as well.[20,21]

In our previous study, dendrimer-conjugated podophyllotoxin was reported to exert minimal side effects and had improved potency at higher doses, possibly due to the sustained release of the nanodevice (DPODO). In addition, tumour inhibition in skin papilloma through anti-inflammatory and apoptotic activity were also reported.[22] Since inflammation and fibrogenesis are major factors in the progression of hepatocellular carcinoma, the present investigation is focused on studying the effect of DPODO on the inflammatory and fibrogenic markers modulating HCC progression.

2.   Results

2.1   Synthesis and characterization

The synthesis of the dendrimer-conjugated podophyllotoxin (shown in Fig. 1A) was followed by characterization through NMR and MALDI-TOF. The characterization outcome indicates the purity of the compounds and conjugated podophyllotoxin
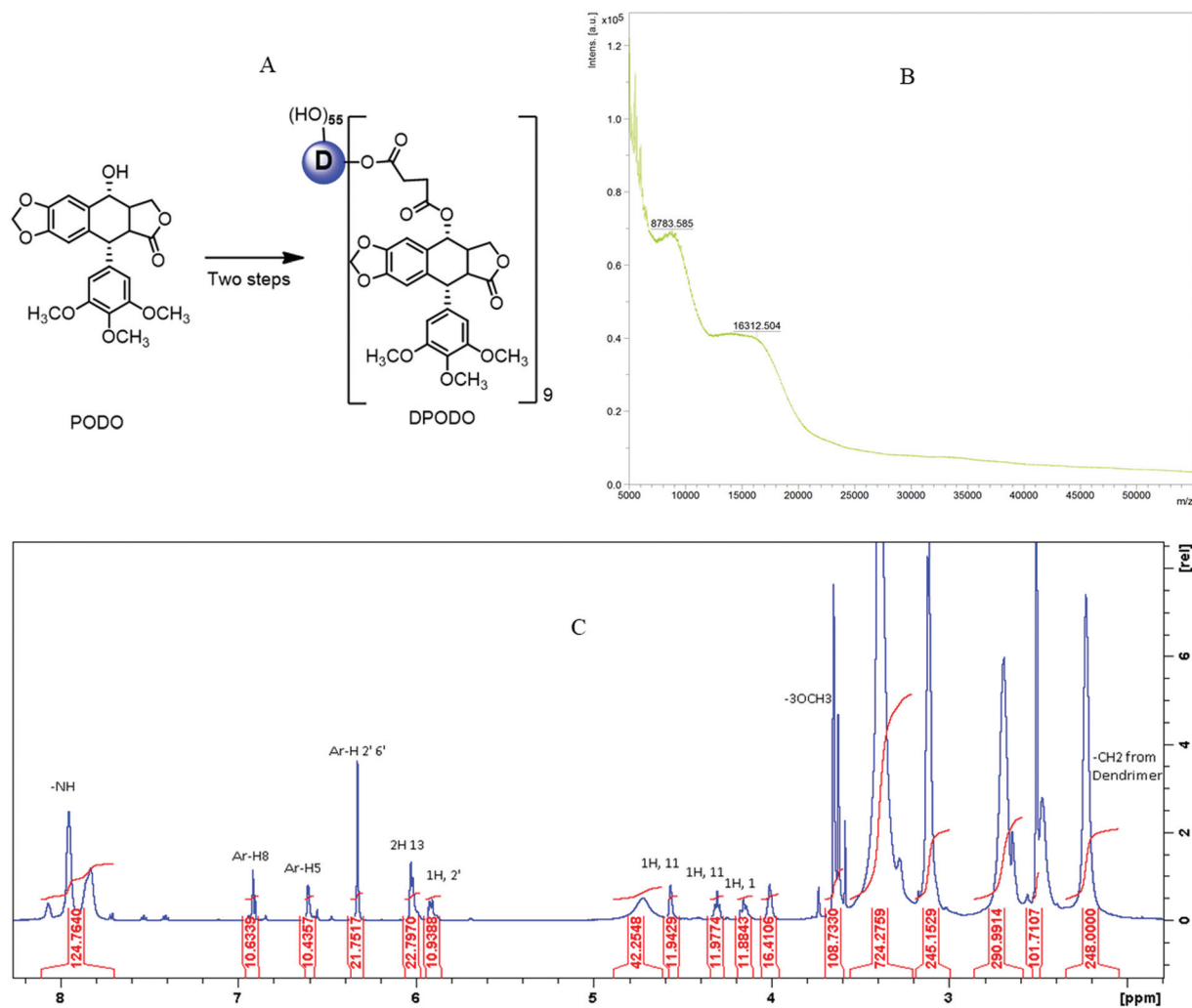

Fig. 1   (A) Synthesis scheme of DPODO, (B) molecular weight determination of DPODO in MALDI-TOF, and (C) ^{1}H-NMR characterization of DPODO in DMSO-d6 solvent.
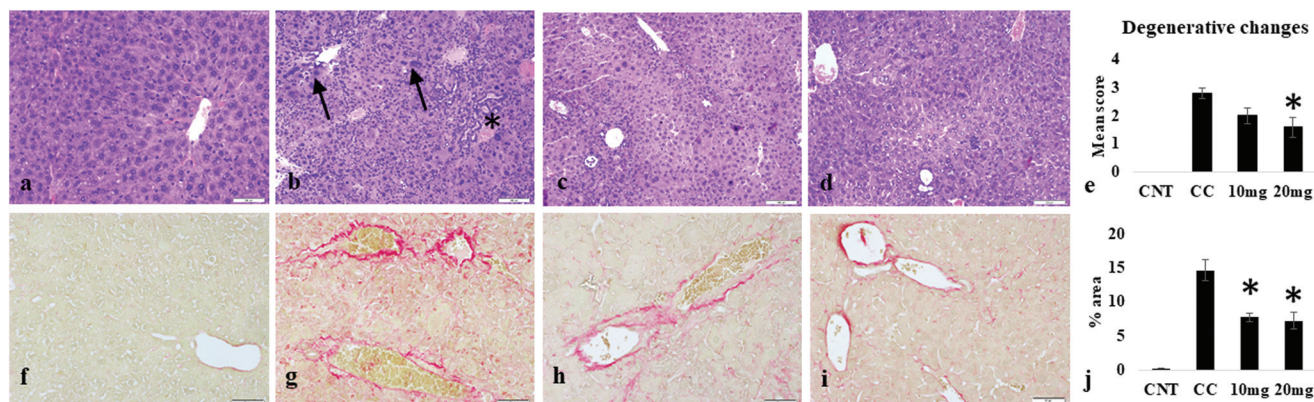
Fig. 2 Histopathological changes in the liver tissue of different groups. (a) Liver in the control group (CNT) showing normal structure; (b) carcinogen control (CC) group showing bile duct hyperplasia (star), karyomegaly (arrow) and degenerative changes; (c, d) liver tissue in groups treated with 10 mg and 20 mg, respectively; (e) mean score of degenerative changes in different groups; (f) picrosirius-stained normal liver with minimal fibrous tissue; (g) fibrous tissue deposition in CC group, (h) 10 mg kg^{-1} group, and (i) 20 mg kg^{-1} group; (j) mean fibrotic area (%) in livers of different groups. $p < 0.05$ as compared to CC.

molecules in the conjugates. Both spectroscopy techniques reflected that 9 molecules of the podophyllotoxin are conjugated to the dendrimer. The spectral data are presented in Fig. 1B and C.

2.2 Body weight

Body weights of mice were taken at weekly intervals. The body weights of different groups were compared at the start of the experiment, on the 10th week, and on the 16th week. The DENA treatment significantly ($p < 0.05$) lowered the body weights in mice by the 10th and 16th weeks. However, no significant improvement was observed by the 16th week in the body weights of mice treated with DPODO (10 mg and 20 mg; ESI, Fig. S1†).

2.3 Effect of DPODO on liver histopathology

The control group showed normal liver histology with regularly arranged hepatocytes and associated structures. The DENA-induced injury in the carcinogen control group led to disarrangement of hepatic architecture, along with many degenerative changes. Hepatocytes of varying sizes with nuclear atypia were observed. Proliferation of bile ducts, marked anisocytosis, anisokaryosis and karyomegaly were well evident. Focal to multifocal proliferation of mononuclear cells was also prominent in the liver parenchyma. The extent of liver degenerative changes was reduced by DPODO treatment at both 10 mg kg^{-1} and 20 mg kg^{-1} dose as compared to the carcinogen control group. However, the effect was found significant ($p < 0.05$) only in the 20 mg kg^{-1} group (Fig. 2a–e).

2.4 Effect of DPODO on fibrous tissue deposition

DENA treatment induced fibrous tissue deposition in the liver, which was stained with picrosirius stain. The control group showed very little fibrous tissue around the blood vessels, but a significant increase ($p < 0.001$) in fibrous deposition was observed in the carcinogen control group as compared to the

control group. The DPODO treatment at 10 and 20 mg kg^{-1} significantly ($p < 0.001$) lowered the extent of fibrous connective tissue deposition in the liver as compared to the carcinogen control group (Fig. 2f–j).

2.5 Effect of DPODO on IL-6 levels

IL-6, a multifunctional proinflammatory cytokine, is associated with various inflammatory disorders. Acute and chronic liver diseases are responsible for elevated serum and intrahepatic levels of IL-6. The DENA treatment significantly increased IL-6 levels in the carcinogen control group. On the other hand, treatment with DPODO at 10 and 20 mg kg^{-1} significantly lowered the levels of IL-6 as compared to the carcinogen control group. This might indicate the anti-inflammatory role of DOPDO in the HCC (Fig. 3).

2.6 Effect of DPODO on NF-κB levels

A transcription factor, NF-κB, has been supposed to be involved in cancer development, forming a pivotal link between inflammation and cancer. The DENA treatment sig-
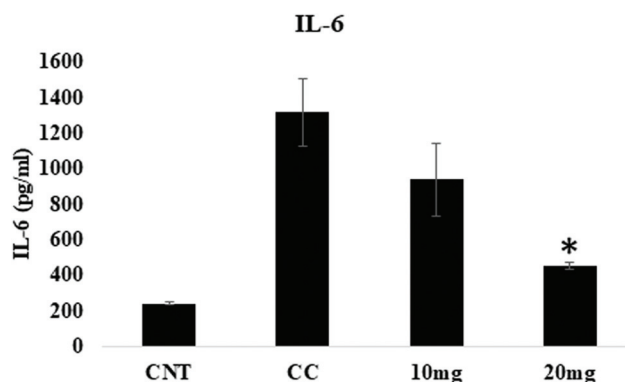

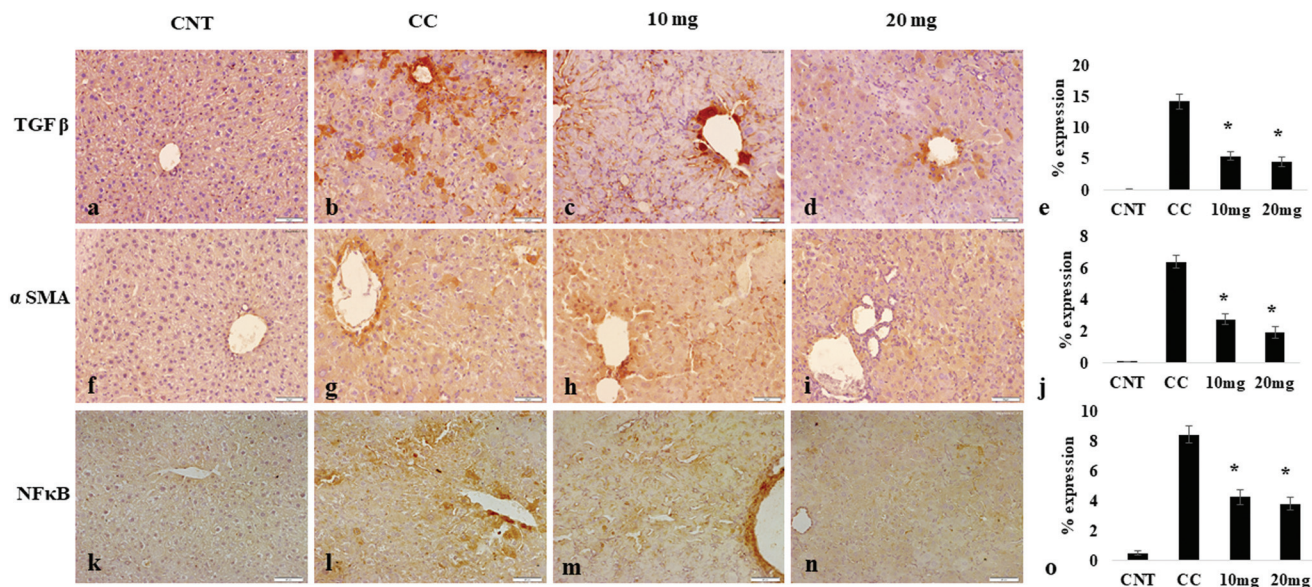**Fig. 3** Effect of DPODO treatment on IL6 levels in serum of different groups.

Fig. 4 Effect of DPODO treatment on the expression of TGF-β (a–d); α-SMA (f–i), and NF-κB (k–n) in liver tissues of different groups. Graphs (e, j, o) showing the comparison of TGFβ, αSMA and NF-κB expressions in different groups, respectively. *$p < 0.05$ as compared to CC.
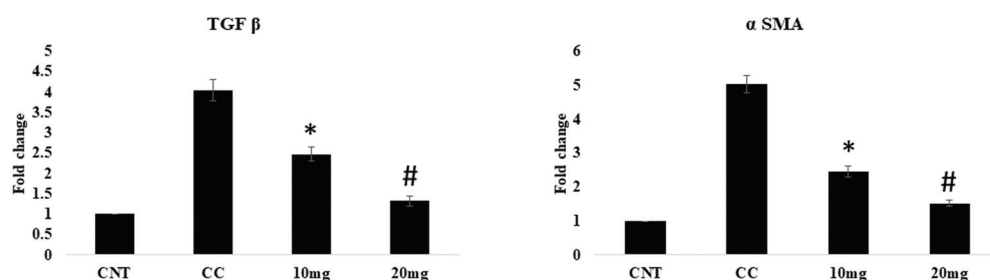

Fig. 5 Effect of DPODO treatment on the mRNA levels of TGF-β and α-SMA in the liver tissue of different groups. *$p < 0.05$ as compared to CC; #$p < 0.05$ as compared to 10 mg kg^{-1} group.

nificantly increased the expression of NF-κB in liver tissues of the carcinogen control group. However, DPODO treatment at 10 mg kg^{-1} and 20 mg kg^{-1} significantly lowered the liver NF-κB expression as compared to the carcinogen control group (Fig. 4).

2.7 Effect of DPODO on α-SMA and TGF-β1 levels

α-SMA and TGF-β play important role in the progression of fibrosis. The effect of DPODO on α-SMA and TGF-β expression in the liver was studied using immunohistochemical analysis (IHC; Fig. 4). The liver tissues showed significantly increased expression of α-SMA and TGF-β in the carcinogen control group as compared to normal. However, significant reduction was observed in the levels of α-SMA and TGF-β in liver tissue of the 10 and 20 mg kg^{-1} treatment groups.

The levels of α-SMA and TGF-β in the liver were further assessed by RT-qPCR and found to be significantly ($p < 0.001$) increased in the carcinogen control as compared to the naïve group. The DPODO treatment at 10 mg kg^{-1} ($p < 0.001$) and 20 mg kg^{-1} ($p < 0.001$) dose significantly reduced the levels of

α-SMA and TGF-β in liver tissue in a dose-dependent manner (Fig. 5).

3. Discussion

Podophyllotoxin is an aryl tretralin lactone isolated from the genera *Podophyllum*. Due to its high toxicity and side effects, such as enteritis and depression of the central nervous system, the use of this compound is limited to a local antiviral agent. However, its semi-synthetic derivatives etoposide, teniposide and etopophos are significant anticancer agents due to their ability to inhibit the enzyme topoisomerase II.[23] In our previous studies, we have reported that dendrimer-conjugated podophyllotoxin possesses increased bioavailability and reduced toxicity in comparison to its precursor molecule. It was also found to be efficacious against skin tumour by inducing cell death and reducing inflammation.[22] Treatment with the DPODO conjugate has also been shown to induce cell cycle arrest and tubulin depolymerisation, as well as escalate cell

death as compared to the free drug.[10] In the present investigation, we hypothesized that DPODO can also be effective against DENA-induced hepatocellular carcinoma.

In the body, DENA is metabolized into its active ethyl radical metabolites by the action of CYP2E1 cytochrome, which metabolizes low molecular chemicals, including carcinogens and toxicants.[24] The reactive metabolites of nitrosamine cause alteration in the enzymes involved in DNA repair or replication, leading to the formation of alkyl DNA adducts and chromosomal aberrations, ultimately ending in carcinogenesis. DENA is reported to potentiate liver injury, possibly due to deficiency of carnitine, which is known to actively participate in the biosynthesis of fatty acids and mitochondria-dependent apoptosis.[22,25,26]

In the present study, no significant effect of DPODO treatment was observed on body weight, which might be due to severe alteration of liver function by DENA, leading to impaired body weight gain in rats. DENA administration has been associated with morphological variation in hepatocytes, leading to their transformation into neoplastic cells.[27] Lesions in liver tissues have been reported earlier to be due to elevated levels of liver enzymes causing damage to the tissue.[28,29] The histopathological studies showed that DENA treatment caused complete distortion of liver histology and led to proliferation of bile ducts, anisocytosis, anisokaryosis and karyomegaly. The infiltration of inflammatory cells was also observed along with the degenerative changes. The DPODO treatment reduced the extent of degenerative changes in the liver tissue and, to an extent, restored the normal architecture of the liver. In an earlier report, podophyllotoxin also successfully reduced interstitial edema, inflammatory cell intrusion, and congealing of the alveolar wall in irradiated lungs.[30] DPODO treatment was also reported to reduce hyperkeratosis, epidermal hyperplasia, and pearl body formation in DMBA-TPA-induced skin tumour.[22]

IL-6 is synthesized primarily by macrophages, fibroblasts, endothelial cells, *etc.*, and plays a role in the body's response towards injury or infection. Serum levels of IL-6 are used as a diagnostic marker in clinical practice due to their exacerbation after inflammation.[31] There is a correlation between IL-6 signalling and HCC progression.[32] The detrimental role of IL-6 is due to trans-signalling of IL-6 leading to DNA damage and thereby causing endothelial cell promotion and enhanced tumor growth. In the present study, we observed elevated levels of IL-6 in serum due to liver inflammation. DENA treatment might have induced the release of IL-1α from hepatocytes, which in turn activated Kupffer cells to produce IL-6. DPODO was able to reduce the levels of IL-6 effectively in the mice, indicating the anti-inflammatory effect of the molecule. IL-6 also regulates NF-κB expression in hepatocytes, which leads to HCC development.[33,34] In the present study, the DENA-induced increased expression of NF-kB in liver tissue was significantly inhibited by DPODO treatment. Similar results were observed in our previous study, where DPODO treatment against squamous cell carcinoma showed efficacy by altering the expression of NF-κB and inducing apoptosis.[22]

NF-κB is a transcriptional regulator and an important link between inflammation and HCC; therefore, suppression of the NF-κB signalling pathway may influence effective anti-cancer treatment.[35] TGF-β1 has been regarded as a key factor in hepatic damage by regulating the induction, proliferation and differentiation of epithelial cells and collagen-producing myofibroblasts, leading to liver cirrhosis and HCC.[36] TGF-β, as a pro-fibrogenic factor, is closely related to liver fibrosis by activating Smad2/3 and thereby promoting the growth of HCC.[37,38] It also modulates diverse cytokines such as TNF-α and IL-1β/13, stellate cell proliferation, and increased production of extracellular matrix.[39] Similarly, proliferation of stellate cells and their differentiation is closely associated with TGF-β and the development of hepatic fibrosis progression through α-SMA.[40] Although stellate cells are normally positive for α-SMA, its expression is significantly marked in chronic damage due to stimulation of stellate cells, making it a reliable marker. In the present study, induced expression of TGF-β and α-SMA genes were observed in the HCC, which was further confirmed by studying protein expression in the liver tissues. DPODO treatment significantly lowered the expression of these genes, which indicates its efficacy against the progression of HCC by inhibiting liver fibrosis. In an earlier study, podophyllotoxin in combination with rutin significantly decreased the expression of TGF-β1 in lung fibrosis.[30] Other reports also show that the use of lignans reduced the fibrosis by countering the pro-inflammatory and fibrogenic cyotkines.[41]

4. Experimental

4.1 Chemicals

DENA, α-Sirius red, smooth muscle actin (αSMA), and TGF-β antibodies were procured from Sigma-Aldrich, St Louis, Missouri, USA. IL-6 ELISA kit was from Raybiotech Inc., Norcross, Georgia, and kits for immunohistochemistry were from Vectorlabs, California, USA. RT-qPCR kit was obtained from Thermo Fisher Scientific, Massachusetts, USA. NF-κB antibody was from Life Technologies, California, USA. Picric acid for picrosirius red staining was from SDFCL, Mumbai, India.

4.2 Chemical synthesis

The conjugate DPODO was synthesized following our previous report.[13,22] Briefly, a suspension of succinic anhydride (0.3 g, 3.02 mmol) in anhydrous CHCl$_3$ (5.0 mL) was added to a mixture of PODO (0.5 g, 1.2 mmol), DMAP (0.176 g, 1.44 mmol), and Et$_3$N (191 μl, 3.0 mmol) in anhydrous CHCl$_3$ (10 mL) at room temperature and stirred for 3 h. The volatiles were evaporated under vacuum, and the product was purified through column chromatography (95 : 5, CH$_2$Cl$_2$: MeOH). The white product was the isolated PODO-linker (0.43 g, 69%). The PAMAM dendrimer (D generation four, ethylenediamine core; 0.3 g, 0.021 mmol) was dissolved in dry DMF (5.0 mL) and then added to a mixed solution of PODO-linker (0.195 g, 0.387 mmol), Py-Bop (218.6 mg, 0.42 mmol), and DIEA

(100 μL) in DMF (10.0 mL), and the mixture was stirred for another 18 hours at room temperature in the presence of nitrogen. The resulting reaction mixture was purified through dialysis membrane (3 kDa), dialyzed against DMF, and the product was re-dissolved in water and lyophilized, producing a white pure solid product (0.40 g). ^{1}H NMR and MALDI-TOF (Fig. 1 and 2) were used to characterize the purified final compound DPODO. ^{1}H NMR (600 MHz, DMSO-d6): 8.07–7.69 (m, amide -NH from D), 6.90 (s, 1H, Ar-H-8), 6.60 (s, 1H, Ar-H-5), 6.32 (s, 2H, Ar-H-2′ and 6′), 6.02 (m, 2H, H-13), 5.93 (m, 1-H, H-2), 4.72 (from D), 4.56 (m, 1H, H-11), 4.30 (1H, H-11), 4.15 (1H, H-1), 4.0 (s), 3.65 (s, 6H, -OCH3 -H), 3.63 (s, 3H, -OCH3-H), 3.39 (m, broad peak), 3.12 (m, broad peak), 2.69 (m, broad peak from dendrimer, H-2, H-3, and proton from PODO linker (a and b)), 2.47 (m, dendrimer peak), 2.23 (m, dendrimer –CH$_2$).

4.3 Animals

The study was carried out on six-week-old adult Swiss albino male mice (22 ± 2 g) procured from the animal facility of the CSIR-Institute of Himalayan Bioresource Technology, Palampur, India. The animals were kept at the optimum temperature of 22 ± 5 °C under alternating 12 h light/dark cycles and 35%–40% humidity. Pelleted feed and drinking water were provided *ab libitum* to the animals. Handling of animals and the experimental protocol were conducted in accordance with the CPCSEA guidelines, and the protocol was approved by the Institutional Animal Ethical Committee (IAEC).

4.4 Experimental protocol

Four groups with five mice each were used in the study. Group I served as the naïve mice, which received normal drinking water for 16 weeks. The rest of the groups (II–IV) were exposed to 0.01% DENA in their drinking water for 16 weeks for the initiation of hepatocellular carcinoma (HCC). Groups III and IV received DPODO treatment at 10 mg kg^{-1} and 20 mg kg^{-1} dose, respectively, after the 10th week until the 16th week. Group II served as carcinogen control (0.01% DENA). The body weights of mice were measured weekly. At the end of the study, liver tissue was taken, and a part of it was stored at −80 °C for the expression analysis; the rest was stored in 10% neutral buffered formalin for further histopathological and immuno-histochemical studies.

4.5 Histopathology

Animals were euthanized at the end of the experiment, and liver tissues were collected in 10% neutral-buffered formalin. The liver tissues were dehydrated and cleared using xylene for histopathological study. Paraffin-embedded tissues were trimmed, sectioned at 3–5 μm, and processed further for hematoxylin and eosin staining. The slides were examined using bright field microscope (Olympus BX53F). The microscopic changes in the liver, including anisocytosis, karyomegaly, inflammation and necrosis were graded as no changes – 0; mild/focal changes – 1; moderate/multifocal changes – 2; and severe/diffuse changes – 3.[28]

4.6 Picrosirius stain

Fibrous tissue deposition in the liver was assessed by picrosirius stain; the paraffin-embedded and 4 μm tissue sections were firstly stained with Weigert's hematoxylin followed by incubation with picrosirius red for 1 h. After removing the excess stain with an acetic acid/water (5 : 1000) solution, the sections were dehydrated in ethanol, cleared in xylene and mounted with DPX mountant for observation. The stained slides were analyzed under bright field microscope (Olympus BX53F), and the fibrotic changes were quantified using ImageJ software.

4.7 Immunohistochemistry

Expression of proteins related to the inflammatory and fibrosis pathway was studied through immunohistochemistry. Tissue sections (5 μm) from the liver were deparaffinized and hydrated, then the antigen was retrieved using sodium citrate (pH 6.0). ImmPRESS Excel staining kit was used for the rest of procedure, as described previously.[22] α-SMA, TGF-β and NF-κB from rabbit were used for the study at 1 : 50–1 : 100 dilution in PBS. Observations were done under Olympus BX53F bright field microscope (Olympus), and expression of respective antibodies was evaluated by ImageJ software.

4.8 ELISA

Serum samples were used to quantify IL-6 through ELISA to evaluate cytokine release. IL-6 direct ELISA kit from RayBiotech was used with coated IL-6 antibody and biotinylated anti-IL-6 antibody following manufacturer's instructions. The assay was performed in duplicate.

4.9 Total RNA isolation and RT-qPCR

The liver sections stored in −80 °C were subjected to Trizol for isolation of total RNA. 100 mg of liver tissue was homogenized in 100 ml of Trizol (Tri reagent, Sigma-Aldrich). The addition of 0.2 ml of chloroform resulted in the separation of nucleic acid into the aqueous phase after a cool spin-down for 15 min at 4 °C. RNA in the aqueous layer was separated using isopropanol, and the pellet was washed with 70% ethanol, dried at room temperature and solubilized in RNase-free water. Quantity and purity of RNA were measured using nanodrop (Thermo Fisher Scientific, United States).

For RT-qPCR, 2 μg of RNA was converted into cDNA as per manufacturer instructions (Applied Biosystems, USA), and Primer express 3.0 software was used to synthesize primers specific to target genes (Applied Biosystems, USA) as follows:

α-SMA F-ACTGGGACGACATGGAAAAG
    R-GTTCAGTGGTGCCTCTGTCA
TGF-β F-GAGAAGAACTGCTGTGTGCG
    R-GTGTCCAGGCTCCAA ATATAG
GAPDH F-TCACTCAAGATTGTCAGCAATGC
    R-TCATGAGCCCTTCCACAATG.

The reaction was carried out in 8-tube strips using the StepOnePlus™ RT-qPCR system (Applied Biosystems, United

States). GAPDH was used as the constitutive gene for normalization of the target gene expression.

4.10 Statistical analysis

All the results were expressed as a mean ± standard error. The significance of difference for different parameters was analyzed using one-way analysis of variance (ANOVA) followed by Tukey's *post hoc* test. The results were regarded as significant at $P < 0.05$.

5. Conclusion

In conclusion, the study showed the therapeutic effect of DPODO against HCC in mice. The efficacy of DPODO might be due to the fact that dendrimer conjugation improved the stability and sustainability for a prolonged time in the physiological condition, and increased the sustained release capacity as well as the tissue penetrating effect. In addition, the compound efficiently lowered the inflammatory and fibrogenic factors in the liver, which are the key elements in the progression of HCC. Overall, DPODO could be one of the treatment options for liver cancer in the future; however, more detailed studies on the mechanism and long-term safety of the molecule are required.

Conflicts of interest

There are no conflicts of interest to declare.

Acknowledgements

References

1 J. U. Marquardt, J. B. Andersen and S. S. Thorgeirsson, Functional and genetic deconstruction of the cellular origin in liver cancer, *Nat. Rev. Cancer*, 2015, **15**(11), 6536–6567.

2 L. A. Torre, F. Bray, R. L. Siegel, J. Ferlay, J. Lortet-Tieulent and A. Jemal, Global cancer statistics, 2012, *CA-Cancer J. Clin.*, 2015, **65**(2), 87–108.

3 P. J. Zamor, A. S. deLemos and M. W. Russo, Viral hepatitis and hepatocellular carcinoma: etiology and management, *J. Gastrointest. Oncol.*, 2017, **8**(2), 224–229.

4 L. Tessitore, Hepatocellular carcinoma is induced by a sub-necrogenic dose of diethylnitrosamine in previously fasted-refed rats, *Nutr. Cancer*, 1998, **32**(1), 49–54.

5 M. K. Pulatova, V. L. Sharygin, G. T. Rikhireva, A. I. Sergeev, Y. I. Mitrokhin and I. N. Todorov, The most important stages of the mechanism of action in vivo of carcinogen diethylnitrosoamine and its effect on the synthesis of RNA, proteins, DNA, and deoxyribonucleotides, *Biofizika*, 2011, **56**(4), 748–759.

6 D. Dimitroulis, C. Damaskos, S. Valsami, S. Davakis, N. Garmpis, E. Spartalis, A. Athanasiou, D. Moris, S. Sakellariou, S. Kykalos and G. Tsourouflis, From diagnosis to treatment of hepatocellular carcinoma: An epidemic problem for both developed and developing world, World J, *Gastroenterol.*, 2017, **23**(29), 5282.

7 M. Gordaliza, P. A. Garcıa, J. M. Del Corral, M. A. Castro and M. A. Gómez-Zurita, Podophyllotoxin: distribution, sources, applications and new cytotoxic derivatives, *Toxicon*, 2004, **44**(4), 441–459.

8 Y. Q. Liu, L. Yang and X. Tian, Podophyllotoxin: Current perspectives, *Curr. Bioact. Compd.*, 2007, **3**, 37–66.

9 M. A. Papież, W. Krzyściak, K. Szade, K. Bukowska-Straková, M. Kozakowska, K. Hajduk, B. Bystrowska, J. Dulak and A. Jozkowicz, Curcumin enhances the cytogenotoxic effect of etoposide in leukemia cells through induction of reactive oxygen species, *Drug Des., Dev. Ther.*, 2016, **10**, 557–570.

10 U. H. Sk, D. Dixit and E. Sen, Comparative study of microtubule inhibitors–estramustine and natural podophyllotoxin conjugated PAMAM dendrimer on glioma cell proliferation, *Eur. J. Med. Chem.*, 2013, **68**, 47–57.

11 F. Cavalli, L. Tschopp, A. Gerber, R. W. Sonntag, H. J. Ryssel and K. W. Brunner, Therapiersultate mit VP 16.213 allein oder kombiniert mit 5-fluorouracil beim leberzell karzinom (hepatoma), *Schweiz. Med. Wochenschr.*, 1977, **107**, 1960–1966.

12 M. Yoshino, N. Okazaki, T. Yoshida, Y. Kanda, M. Miki, H. Oda, Y. Sasagawa, S. Hayashi and N. Hashimoto, A phase II study of etoposide in patients with hepatocellular carcinoma by the Tokyo Liver Cancer Chemotherapy Study Group, *Jpn. J. Clin. Oncol.*, 1989, **19**(2), 120–122.

13 U. H. Sk, S. P. Kambhampati, M. K. Mishra, W. G. Lesniak, F. Zhang and R. M. Kannan, Enhancing the efficacy of Ara-C through conjugation with PAMAM dendrimer and linear PEG: a comparative study, *Biomacromolecules*, 2013, **14**(3), 801–810.

14 U. H. Sk and C. Kojima, Dendrimers for theranostic applications, *Biomol. Concepts*, 2015, **6**(3), 205–217.

15 V. Patial, S. Sharma and U. H. Sk, dendrimer conjugated estramustine nanocrystalline 'dendot': An effective inhibitor of Dmba-tpa induced papilloma formation in mouse, *Eur. J. Pharm. Sci.*, 2017, **109**, 316–323.

16 K. Madaan, S. Kumar, N. Poonia, V. Lather and D. Pandita, Dendrimers in drug delivery and targeting: Drug-dendrimer interactions and toxicity issues, *J. Pharm. BioAllied. Sci.*, 2014, **6**(3), 139–150.

17 K. M. Kitchens, A. B. Foraker, R. B. Kolhatkar, P. W. Swaan and H. Ghandehari, Endocytosis and interaction of poly (amidoamine) dendrimers with Caco-2 cells, *Pharm. Res.*, 2007, **24**(11), 2138–2145.

18 V. S. Talanov, C. A. Regino, H. Kobayashi, M. Bernardo, P. L. Choyke and M. W. Brechbiel, Dendrimer-based nanoprobe for dual modality magnetic resonance and fluorescence imaging, *Nano Lett.*, 2006, **6**(7), 1459–1463.

19 C. C. Lee, J. A. MacKay, J. M. Fréchet and F. C. Szoka, Designing dendrimers for biological applications, *Nat. Biotechnol.*, 2005, **23**(12), 1517–1526.

20 I. Jatczak-Pawlik, M. Gorzkiewicz, M. Studzian, D. Appelhans, B. Voit, L. Pulaski and B. Klajnert-Maculewicz, Sugar-modified poly (propylene imine) dendrimers stimulate the NF-κB pathway in a myeloid cell line, *Pharm. Res.*, 2017, **34**(1), 136–147.

21 P. Kesharwani, S. Banerjee, U. Gupta, M. C. I. M. Amin, S. Padhye, F. H. Sarkar and A. K. Iyer, PAMAM dendrimers as promising nanocarriers for RNAi therapeutics, *Mater. Today*, 2015, **18**(10), 565–572.

22 U. H. Sk, V. Patial and S. Sharma, A low toxic synthetic dendrimer conjugated podophyllotoxin nanodevice with potent antitumor activity against the DMBA/TPA induced mouse skin carcinogenesis model, *Toxicol. Res.*, 2015, **4**(5), 1204–1213.

23 M. Yousefzadi, M. Sharifi, M. Behmanesh, E. Moyano, M. Bonfill, R. M. Cusido and J. Palazon, Podophyllotoxin: current approaches to its biotechnological production and future challenges, *Eng. Life Sci.*, 2010, **10**(4), 281–292.

24 J. Gao, Z. Wang, G. J. Wang, H. X. Zhang, N. Gao, J. Wang, C. E. Wang, Z. Chang, Y. Fang, Y. F. Zhang and J. Zhou, Higher CYP2E1 activity correlates with hepatocarcinogenesis induced by diethylnitrosamine, *J. Pharmacol. Exp. Ther.*, 2018, **365**(2), 398–407.

25 S. S. Al-Rejaie, A. M. Aleisa, A. A. Al-Yahya, S. A. Bakheet, A. Alsheikh, A. G. Fatani, O. A. Al-Shabanah and M. M. Sayed-Ahmed, Progression of diethylnitrosamine-induced hepatic carcinogenesis in carnitine-depleted rats, *World J. Gastroenterol.*, 2009, **15**(11), 1373–1380.

26 T. Furuno, T. Kanno, K. Arita, M. Asami, T. Utsumi, Y. Doi, M. Inoue and K. Utsumi, Roles of long chain fatty acids and carnitine in mitochondrial membrane permeability transition, *Biochem. Pharmacol.*, 2001, **62**(8), 1037–1046.

27 F. G. Zaki, Ultrastructure of altered hepatocytes induced by diethylnitrosamine (DENA), *Toxicol. Pathol.*, 1982, **10**(2), 50–62.

28 V. Patial, S. Mahesh, S. Sharma, K. Pratap, D. Singh and Y. S. Padwad, Synergistic effect of curcumin and piperine in suppression of DENA-induced hepatocellular carcinoma in rats, *Environ. Toxicol. Pharmacol.*, 2015, **40**(2), 445–452.

29 R. Khan, I. Kazmi, M. Afzal, F. A. Al Abbasi, G. Mushtaq, A. Ahmad, V. Kumar and F. Anwar, Fixed dose combination therapy loperamide and niacin ameliorates diethylnitrosamine-induced liver carcinogenesis in albino Wistar rats, *RSC Adv.*, 2015, **5**(83), 67996–68002.

30 S. Verma, B. Kalita, S. Bajaj, H. Prakash, A. K. Singh and M. L. Gupta, A combination of Podophyllotoxin and rutin alleviates radiation-induced Pneumonitis and Fibrosis through Modulation of lung inflammation in Mice, *Front. Immunol.*, 2017, **8**, 658.

31 S. Rose-John, IL-6 trans-signaling via the soluble IL-6 receptor: importance for the pro-inflammatory activities of IL-6, *Int. J. Biol. Sci.*, 2012, **8**(9), 1237–1247.

32 J. Bergmann, M. Müller, N. Baumann, M. Reichert, C. Heneweer, J. Bolik, K. Lücke, S. Gruber, A. Carambia, S. Boretius and I. Leuschner, IL-6 trans-signaling is essential for the development of hepatocellular carcinoma in mice, *Hepatology*, 2017, **65**(1), 89–103.

33 R. F. El-Folly, R. H. El-Kabarity and N. A. Arafa, Assessment of the role of interleukin-6 in diagnosis of hepatocellular carcinoma, *Egypt. J. Immunol.*, 2010, **17**(2), 11–22.

34 D. Schmidt-Arras and S. Rose-John, IL-6 pathway in the liver: from physiopathlogy to therapy, *J. Hepatol.*, 2016, **64**(6), 1403–1415.

35 D. A. Mann and F. Oakley, NF-κB: a signal for cancer, *J. Hepatol.*, 2005, **42**(4), 610–611.

36 S. Dooley and P. Ten Dijke, TGF-β in progression of liver disease, *Cell Tissue Res.*, 2012, **347**(1), 245–256.

37 M. Mikula, V. Proell, A. N. M. Fischer and W. Mikulits, Activated hepatic stellate cells induce tumor progression of neoplastic hepatocytes in a TGF-β dependent fashion, *J. Cell. Physiol.*, 2006, **209**(2), 560–567.

38 L. Yang, Y. S. Roh, J. Song, B. Zhang, C. Liu, R. Loomba and E. Seki, Transforming growth factor beta signaling in hepatocytes participates in steatohepatitis through regulation of cell death and lipid metabolism in mice, *Hepatol.*, 2014, **59**(2), 483–495.

39 B. Dewidar, J. Soukupova, I. Fabregat and S. Dooley, TGF-β in hepatic stellate cell activation and liver fibrogenesis: updated, *Curr. Pathobiol. Rep.*, 2015, **3**(4), 291–305.

40 X. K. Zhao, L. Yu, M. L. Cheng, P. Che, Y. Y. Lu, Q. Zhang, M. Mu, H. Li, L. L. Zhu, J. J. Zhu and M. Hu, Focal adhesion kinase regulates hepatic stellate cell activation and liver fibrosis, *Sci. Rep.*, 2017, **7**(1), 4032.

41 R. Tahamtan, A. S. Monfared, Y. Tahamtani, A. Tavassoli, M. Akmali, M. A. Mosleh-Shirazi, M. M. Naghizadeh, D. Ghasemi, M. Keshavarz and G. H. Haddadi, Radioprotective effect of melatonin on radiation-induced lung injury and lipid peroxidation in rats, *Cell J.*, 2015, **17**(1), 111.